$\gtrsim 2.51 + 2.90 \gtrsim 5.4$ eV. The resulting asymptotic energy is close to the expected excitation energy so that either there will be discrete structure (nondissociative) in absorption or (dissociative) emission will be observed from the B state of HgCl. In either case, the Hg_2Cl_2 absorption spectrum and resulting emissions should be very different from $HgCl_2$.[24] Therefore, examination of the 200–250-nm region in gas mixtures produced by subliming mercurous chloride may reveal spectroscopic features that can be assigned definitively to Hg_2Cl_2; i.e., it should be possible to discriminate between Hg_2Cl_2 and $HgCl_2$.

V. Conclusion

Two-configuration GVB calculations on the mercurous chloride and fluoride dimers show that both species will have linear mercury-to-mercury geometries (X–Hg–Hg–X). The geometry of the dimer is dictated by a strong covalent Hg–Hg bond, which prevails over the electrostatic interactions of the ionic monomers that favor head-to-tail square geometries. The calculations indicate that Hg_2Cl_2 may be stable in the gas phase. IVO calculations indicate that if Hg_2Cl_2 does exist in the gas phase, it should have distinctive spectroscopic features in the 200–250-nm region that can be used to discriminate between $HgCl_2$ and Hg_2Cl_2.

Acknowledgment. This work was performed under the auspices of the U.S. Department of Energy.

Note Added in Proof: Our preliminary spectroscopic studies of vapor phase Hg_2Cl_2 indicate a broad unstructured band centered at approximately 250 nm and a structured band at about 192 nm. The former band may be due to a transition to the dissociative $1^1\Pi_u$ state and could possibly include a superimposed transition to the $1^1\Sigma_u^+$ state. Much work remains to be done to confirm these tentative assignments. We also note that the mercury 254-nm line is quite prominent suggesting that some disproportionation has occurred.

Intramolecular Proton Tunnelling in the Ground and Lowest Excited Singlet States of 9-Hydroxyphenalenone

R. Rossetti, R. C. Haddon, and L. E. Brus*

Contribution from Bell Laboratories, Murray Hill, New Jersey 07974.
Received April 28, 1980

Abstract: Vibronically resolved fluorescence and fluorescence excitation spectra have been observed for 9-hydroxyphenalenone in solid Ar and Ne. There are strong spectral changes when the phenolic proton is deuterated, implying that the proton motion is coupled to a C_s–C_{2v} rearrangement of the oxygen–carbon molecular framework. In the deuterated compound, a ground-state tunnelling splitting $\Delta = 9 \pm 1$ cm^{-1} is observed. This value increases to 170 cm^{-1} in the excited electronic state. This value, along with other spectral and X-ray structural data, allows us to calculate double-minimum potential energy curve shapes for both ground and excited electronic states by using an approximate theoretical model. The hydride has calculated tunnelling splittings of 127 ± 10 and 617 ± 50 cm^{-1} in ground and excited electronic states, respectively. The calculated ground-state proton-tunnelling times are $\sim$0.13 and $\sim$1.7 ps for the hydride and deuteride, respectively.

Introduction

One interesting question in chemical dynamics involves the interconversion kinetics of molecules that are stable in several equivalent conformations. 9-Hydroxyphenalenone (hereafter 9-HPO), for example, could be postulated to undergo an intramolecular proton transfer between two equivalent cannonical structures as shown in Figure 1.[1] The transformation as drawn principally involves proton motion as the "reaction coordinate", coupled with rearrangement of carbon–oxygen framework bond lengths and angles as the π electrons adjust to the moving proton. A theory of the influence of the π-electron component on potentially symmetrical hydrogen bonds in molecules such as 9-HPO has been recently presented.[2]

9-HPO could be characterized by a double minimum potential as shown in Figure 1 or by a symmetric C_{2v} location for the proton as shown in the lower left corner of the figure. A variety of experiments have provided information about the structure. 9-HPO has a very strong hydrogen bond,[2,3] and the crystalline X-ray structure shows an unusually short O···O distance (2.486 Å).[1] These observations suggest either a C_{2v} structure or "fast" equilibration between two local minima.[1] Deuteron quadrupole studies also support fast exchange between equivalent minima.[4] Gas-phase ESCA spectra show two inequivalent O atoms on the $\sim 10^{-15}$-s time scale.[5] This last experiment shows that the acidic proton remains localized on one O atom for at least several O–H vibrational periods.

The classic experimental method for the analysis of potential energy curve shapes is vibronically resolved electronic spectroscopy. In a molecule as large as 9-HPO, hot bands and rotational structure would normally obscure vibronic structure. Therefore we have investigated the sharp, laser-excited fluorescence and fluorescence excitation spectra of 9-HPO isolated in rare-gas matrices at 4.2 K. This method has been previously applied to other problems of internal structure in large organic species,[6–9] including a study of proton transfer in an excited state of methyl salicylate.[9]

Internal proton-transfer processes may be spectrally resolved when the corresponding rates are too fast to be time resolved with present picosecond laser technology. As illustrated in Figure 1, the vibrationally relaxed "$v = 0$" level of the ground electronic state is doubly degenerate if there are two local minima. Proton tunnelling will split the "$v = 0$" level into two components O^+ and

(1) C. Svensson, S. C. Abrahams, J. L. Bernstein, and R. C. Haddon, *J. Am. Chem. Soc.*, **101**, 5759 (1979).
(2) R. C. Haddon, *J. Am. Chem. Soc.*, **102**, 1807 (1980).
(3) R. C. Haddon, F. Wudl, M. L. Kaplan, J. H. Marshall, R. E. Cais, and F. B. Bramwell, *J. Am. Chem. Soc.*, **100**, 7629 (1978).
(4) L. M. Jackman, J. C. Trewella, and R. C. Haddon, *J. Am. Chem. Soc.*, **102**, 2519 (1980).
(5) R. S. Brown, A. Tse, T. Nakashima, and R. C. Haddon, *J. Am. Chem. Soc.*, **101**, 3157 (1979).
(6) J. Goodman and L. E. Brus, *J. Chem. Phys.*, **69**, 1604 (1978).
(7) A. Baca, R. Rossetti, and L. E. Brus, *J. Chem. Phys.*, **70**, 5575 (1979).
(8) J. Goodman and L. E. Brus, *J. Am. Chem. Soc.*, **100**, 7472 (1978).
(9) J. Goodman and L. E. Brus, *J. Chem. Phys.*, **65**, 1156 (1976).

0002-7863/80/1502-6913$01.00/0

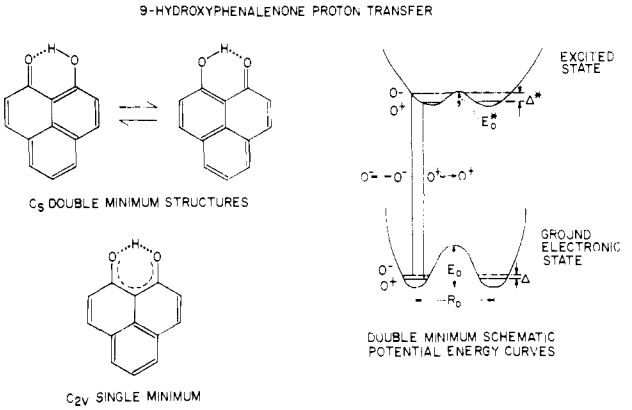

Figure 1. Possible structure for 9-HPO. In the lower left C_{2v} structure, the photon has a single minimum midway between the two O atoms. In the upper left C_s structures and on the right-hand side, the photon oscillates in a double-minimum potential.

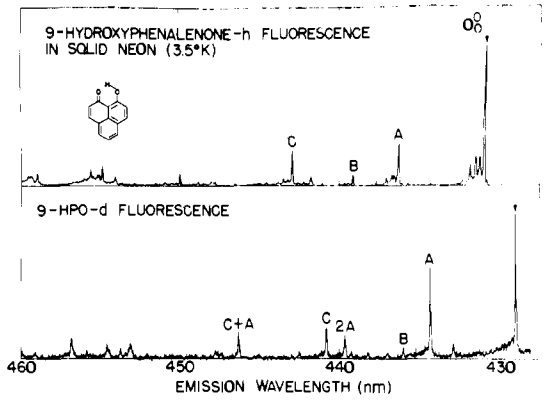

Figure 2. Fluorescence spectra of 9-HPO-*h* and 9-HPO-*d* in solid Ne host. The origin lines O_0^0 are marked with arrows. Letters refer to bands discussed in the text.

O^- with energy separation Δ. A similar process occurs in an excited electronic state, where the splitting Δ^* and proton-transfer barrier E^* could be entirely different. We shall attempt to identify proton-transfer splittings Δ in the electronic absorption and fluorescence of 9-HPO.

Experimental Section

To our knowledge the luminescence and photophysics of 9-HPO have not been previously investigated. We observed wavelength-resolved luminescence of 9-HPO in solid Ne and Ar matrices near 4 K following pulsed, tunable dye laser excitation. The apparatus has been previously described in detail.[9] At room temperature, 9-HPO is a yellow crystalline solid of low ($<10^{-3}$ torr) vapor pressure. We prepared matrices of 9-HPO by flowing rare gas over the compound heated to 50 or 100 C. Vapor molecules of 9-HPO are entrained in the flowing gas and deposited on a Pt surface held at 4 K. Samples with the phenolic proton deuterated were made by dissolving 9-HPO in excess MeOD, evaporation of the solvent, and subsequent matrix deposition of 9-HPO-*d* without exposure to air. The compound is a strong emitter, and spectra were normally obtained with OD1 or OD2 in the laser beam ($\simeq 5 \times 10^{-4}$ J pulses) to avoid saturation in absorption. The inhomogeneous line shape ("distribution of sites") was essentially eliminated in our spectra by the use of narrow spectrometer bandwidths in emission ($\Delta\lambda \simeq 1.0$ Å) and narrow dye lasers ($\Delta\lambda \simeq 0.2$ Å) in excitation.

Observation and Discussion

We concentrate on spectra in solid Ne as experience has shown that neon solvent usually negligibly perturbs a guest molecule from its intrinsic, gas-phase structure. In neon the interaction between the molecule and the solvent is minimized as the host polarizability is very low, and the host compressibility ("softness") is very high.

Both 9-HPO-*h* and 9-HPO-*d* fluoresce strongly without detectable phosphorescence when excited near 4300 Å. Figure 2 shows emission spectra observed for both 9-HPO-*h* and 9-HPO-*d*; the corresponding normalized laser excitation spectra are shown

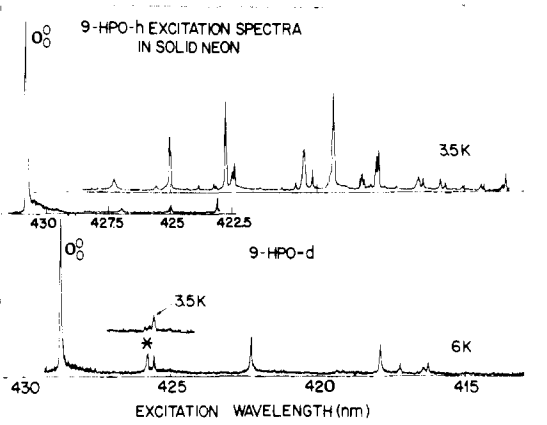

Figure 3. Normalized excitation spectra in Ne host. For 9-HPO-*d*, the asterisk marks the band whose relative intensity increases with temperature. The exhibited 9-HPO-*h* excitation spectrum is composed of two traces. The lower trace has a different wavelength scale from that of the entire figure.

Table I. Analysis of 9-HPO-*h* and 9-HPO-*d* Emission Spectra in Neon[a]

9-HPO-*d*			9-HPO-*h*			
I	*E*, cm^{-1}	ΔE, cm^{-1}	*I*	*E*, cm^{-1}	ΔE, cm^{-1}	comments
8	23 301		7	23 199		
0.5	23 094	210				
5	23 020	284	2.2	22 917	282	A(282)
0.4	22 875	429	0.5	22 769	430	B(430)
0.3	22 760	554				
1.5	22 739	565	0.3	22 632	567	2A
1.7	22 680	625	1.6	22 768	631	C(631)
1.2	22 396	908				C + A
0.7	22 060	1241	0.6	22 213	986	
0.4	22 030	1274	0.4	22 017	1183	
0.5	21 992	1312	0.8	21 975	1224	
0.9	21 885	1419	0.5	21 939	1260	2C for 9-HPO-*h*
0.3	21 774	1530	0.6	21 778	1421	1241 + A for 9-HPO-*d*
0.5	21 721	1583	0.4	21 677	1522	
0.3	21 596	1707				1419 + A

[a] Band labels from Figure 2.

in Figure 3. Each vibronic transition in these spectra consists of a sharp zero phonon line (ZPL) with a negligible phonon wing. This is normally the case when observing delocalized π states in rare-gas solids. The emission spectra are vibrationally relaxed, and the excitation spectra essentially map out the absorption spectra under the resonable assumption of a constant relaxation quantum yield into the fluorescing "$v = 0$" level.

Without an understanding of the ground-state vibrational normal modes, as would come from detailed Raman and infrared studies, we can not attempt a complete vibronic analysis. We instead search for features sensitive to deuteration and discuss the spectra initially in a phenomenological sense.

Tunnelling splittings would best reveal themselves via temperature-dependent features. Suppose that both excited- and ground-state "$v = 0$" levels are split into O^+ and O^- components as in Figure 1. In an allowed electronic transition, only the $O^+ \leftrightarrow O^+$ and $O^- \leftrightarrow O^-$ vibronic members could occur under electric dipole rules. In the unlikely case that the tunnelling splitting were identical in both excited and ground electronic states, then these two lines would be coincident. More probably these two lines will be split by $\Delta - \Delta^*$, and one ($O^- \leftrightarrow O^-$) will show, in both absorption and fluorescence, a reversible temperature dependence as O^- is thermally populated. In Ne and Ar hosts, the maximum practical values of kT are ~ 5 and ~ 20 cm^{-1}, respectively.

There are no detectable, thermally dependent lines in the fluorescence spectra of either isotope. However, there are important isotopic differences. The O_0^0 line ($O^+ \leftrightarrow O^+$) is the most intense feature in both spectra; yet there is a vibronic band labeled

A whose *intensity* is twice as high in the 9-HPO-*d* as in 9-HPO-*h*. The *frequency* of the ground-state vibration corresponding to A is the same in both 9-HPO-*d* and 9-HPO-*h*, as shown in Table I. Thus we have a situation where the acidic proton is not involved in the reduced mass of this particular vibration. Nevertheless, isotopic substitution causes a different displacement along this normal mode between the excited and ground states. This demonstrates that the time averaged molecular proton (deuteron) position is coupled to geometrical changes along (at least) one other normal mode as is postulated in Figure 1. Very recently we have observed a similar coupling of the proton motion to another mode in the intramolecular tunnelling of tropolone.[10] In that case the mode is suspected to be a C–C–O bending motion in the chelate moiety, effectively modulating the O···O distance. The fluorescence involves other characteristic ground-state modes of 282, 430, and 628 cm^{-1} as shown in Table I.[11]

We discuss the vibrational structure as due to totally symmetric Franck–Condon modes, implying that appearance of a vibration indicates a shift in structure along that coordinate in the excited state. In order to check this point, we performed photoselection experiments[12,13] measuring the 9-HPO-*h* fluorescence polarization following linearly polarized excitation. This experiment determines the orientation of the fluorescence transition dipole with respect to the absorption transition dipole. The stronger fluorescence bands all show parallel polarization following excitation of any of the stronger Figure 3 adsorptions, including the O_0^0 band. Thus none of these vibronic transitions involves a nontotally symmetric vibration, which via Herzberg-Teller coupling could borrow intensity from a second electronically excited state of different symmetry. This experiment eliminates the possibility that our anomalous vibronic structure observations reflect Herzberg–Teller coupling between two closely lying states as, for example, has been observed in substituted benzaldehydes.[14,15] Normally Herzberg–Teller vibronic bands are observed when the intrinsic $S_0 \rightarrow S_1$ transition dipole is weak. However, in the case of 9-HPO, the intrinsic dipole is strong as shown by a peak decadic absorption coefficient of $\epsilon \simeq 8000$ L/(mol cm) for the O_0^0 band at 4360 Å in hexane solution.

In the excitation spectra, there is one weak feature, whose intensity reproducibly increases with increasing temperature, seen only in the spectra of 9-HPO-*d*. This band lies 160 cm^{-1} *blue* of $O^+ \leftrightarrow O^+$ and is marked with an asterisk in Figure 3. We interpret this line to be the $O^- \rightarrow O^-$ component, appearing weakly as a small fraction of the ground-state population resides in the upper tunnelling component O^- near 7 K. In the limited range of 3.8–7 K in neon, the relative intensity of $O^- \rightarrow O^-$ compared with $O^+ \rightarrow O^+$ implies an activation energy of about 10 cm^{-1}. The fact that $O^- \rightarrow O^-$ lies 160 cm^{-1} blue of $O^+ \rightarrow O^+$ implies that the tunnelling splitting is 170 cm^{-1} in the excited electronic state. In the parent 9-HPO-*h* compound both these splittings will be much larger due to the smaller mass of the proton. Therefore it is reasonable that neither 9-HPO-*h* nor 9-HPO-*d* show thermally dependent features in fluorescence as the upper tunnelling components O^- lie far to high to be thermally populated in the excited state. In the ground electronic state of 9-HPO-*h*, O^- also lies too high to be experimentally observed.

In the next section we will use these data with other structural information to generate probable quantitative potential energy curves for the ground and excited states of 9-HPO. In a qualitative sense, the large increase in the tunnelling splitting in the excited state shows that the excited-state barrier to proton transfer E_0^* is much smaller than E_0. The equilibrium geometry in the excited state is closer to a C_{2v} structure.

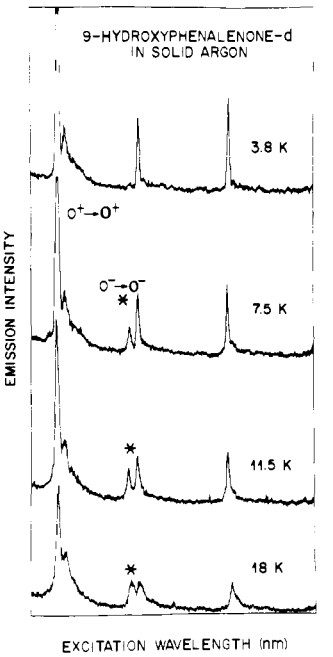

Figure 4. 9-HPO-*d* excitation spectra in argon as a function of temperature. The asterisk marks the temperature-dependent feature ("hot band") $O^- \rightarrow O^-$. Note that the O_0^0 band ($O^+ \rightarrow O^+$) is offscale in the upper two traces.

The Figure 3 excitation spectra show a strong isotopic variation, greater than that observed in fluorescence in Figure 2. The deuteride excitation spectrum is relatively simple, involving 3 prominent lines of 172, 363, and 609 cm^{-1} excited-state frequencies. The hydride spectrum is much richer, containing many lines of weaker vibronic intensity. There is little correspondence between the frequencies, except for a 627-cm^{-1} 9-HPO-*h* line which appears to be analogous to the 609-cm^{-1} 9-HPO-*d* line. Isotopic substitution has totally transformed the excited-state structure as revealed by the absorption spectrum, more so than in any other molecular absorption spectrum known to us. We return to this point in the next section.

We have also studied these spectra in solid argon for two reasons: first to observe the $O^- \rightarrow O^-$ feature over a wider range of temperature and second to see if the 9-HPO tunnelling and vibronic features are dependent upon the environment. Figure 4 shows a portion of the 9-HPO-*d* excitation spectrum including both $O^+ \rightarrow O^+$ and $O^- \rightarrow O^-$. In solid Ar the spectra are shifted about 7 nm to the red, showing a preferential electronic stabilization of the excited state in the more polarizable argon. However, the absorption and fluorescence vibronic structure, and the specific differences between 9-HPO-*h* and 9-HPO-*d*, are almost unchanged in argon. Figure 4 shows the $O^+ \rightarrow O^+$ and its first two vibronic members as in Figure 3. The $O^- \rightarrow O^-$ line appears in the same relative position as in Figure 3; an Arrhenius plot of these data gives an activation energy of 9 ± 1 cm^{-1}. In argon, the $O^- \rightarrow O^-$ line lies 148 cm^{-1} blue of $O^+ \rightarrow O^+$. We conclude that the spectra we observe in solid neon are very close to those of the unperturbed molecule.

Excited- and Ground-State Potential Energy Curves

The data indicate that the phenolic proton motion in ground and excited electronic states is complex. We will make several approximations in order to develop a semiquantitative picture from the available data. We will consider only the O···H···O linear motion, considering it to be a separable normal mode, and use reduced masses of the free proton and deuteron. In actual fact it appears that the wave function is not factorable into an electronic part times a vibrational part, because the π electrons in the carbon–oxygen framework couple to the proton position. It may

(10) R. Rossetti and L. E. Brus, *J. Chem. Phys.*, submitted for publication.
(11) Figure 2 shows that 9-HPO-*h* exhibits structure in the O_0^0 phonon wing in fluorescence but not in the excitation spectra. This structure is absent in the corresponding 9-HPO-*d* spectra. The structure consists of several maxima separated by tens of wavenumbers. It seems unlikely that ground-state 9-HPO-*h* has a normal mode at such a low frequency. It may be that the proton motion in 9-HPO-*h* is coupled to some resonant lattice phonon motion, which then appears in the phonon wing as a "local phonon".
(12) A. C. Albrecht, *J. Mol. Spectrosc.*, **6**, 84 (1961).
(13) V. E. Bondybey and L. E. Brus, *J. Chem. Phys.*, **64**, 3724 (1976).
(14) I. Ozkan and L. Goodman, *Chem. Phys. Lett.*, **64**, 32 (1979).
(15) A. Despres, V. Lejeune, E. Migirdicyan, and W. Siebrand, *Chem. Phys.*, **36**, 41 (1979).

Table II. Analysis of Excitation Spectra[a]

9-HPO-*d*			9-HPO-*h*		
I	*E*, cm^{-1}	ΔE, cm^{-1}	*I*	*E*, cm^{-1}	ΔE, cm^{-1}
10	23 301		10	23 199	
1.0	23 141	160*	0.06	23 404	205
1.0	23 473	172	0.6	23 513	314
2.6	23 664	363	1.2	23 620	420
1.9	23 910	609	0.2	23 630	431
0.6	23 948	647	0.2	23 634	435
0.4	24 993	692	0.06	23 742	553
0.8	24 003	702	0.4	23 769	570
			0.2	23 786	587
			1.0	23 826	627
			0.2	23 888	689
			0.1	23 893	694
			0.3	23 908	709
			0.4	23 912	713
			0.2	23 990	791
			0.1	23 998	799
			0.1	24 034	835
			0.6	24 043	844

[a] The 9-HPO-*d* band labeled with a asterisk is temperature dependent as shown in Figures 3 and 4.

Table III. Parameters in the Double-Minimum Potential Energy Curves of 9-HPO[a]

state	Δ(h), cm^{-1}	Δ(d), cm^{-1}	E_0, cm^{-1}	R_0, Å
ground	118	9	4950	0.48
	136	9	12520	0.34
excited	567	170	1468	0.42
	667	170	3047	0.35

[a] Δ(d) is experimentally measured, R_0 is chosen consistent with the X-ray structure,[1] and E_0 and Δ(h) are calculated as described in the text.

also be true that the "reaction coordinate" for the proton transfer will involve some carbon and oxygen atom motion.[16]

A double-minimum potential energy curve can be analytically represented with two independent parameters (A and B) as

$$V(\mathrm{R}) \equiv A(\mathrm{R}^4 - \mathrm{BR}^2) \quad (1)$$

Numerical solutions of the vibrational Schrödinger equation for this potential have been previously tabulated.[17] In the ground electronic state of 9-HPO we have only one datum, Δ(d) = 9 ± 1 cm^{-1}, and thus can not uniquely determine $V(R)$. However, we can make use of the crystalline X-ray structure[1] which yields the O···O distance as 2.486 Å. With use of an O–H bond length of 1.09 Å for a strong hydrogen bond, it has been estimated that the separation between the two potential energy wells is $R \simeq 0.4$ Å.[1] Employing two representative values R_0 = 0.48 Å and R_0 = 0.33 Å in this neighborhood, we have determined quantitative shapes for the proton-transfer potential in Table III. One of these curves appears in Figure 5. We find E = 8200 ± 4200 cm^{-1} and Δ(h) = 127 ± 10 cm^{-1}, with the explicit caveat that the reader must remember the various assumptions built into this simplified analysis. Table III shows that there is a strong correlation between the chosen R_0 and the calculated value of E_0 for a fixed experimental Δ(d). The calculated Δ(h) is much less sensitive to R_0.

In a similar fashion, in the excited state we know Δ^*(d) = 170 cm^{-1}. Table III shows the quantitative potentials which can be constructed here, yielding Δ^*(h) ≡ 617 ± 50 cm^{-1} and E^* = 2250 ± 800 cm^{-1}. Figure 5 shows that E in the excited state is about a factor of 3 lower than in the ground electronic state.

Figure 5 suggests that the v = 1 level of 9-HPO-*h* lies above or near the top of the barrier E. This state should undergo a complicated motion and be strongly coupled to other normal

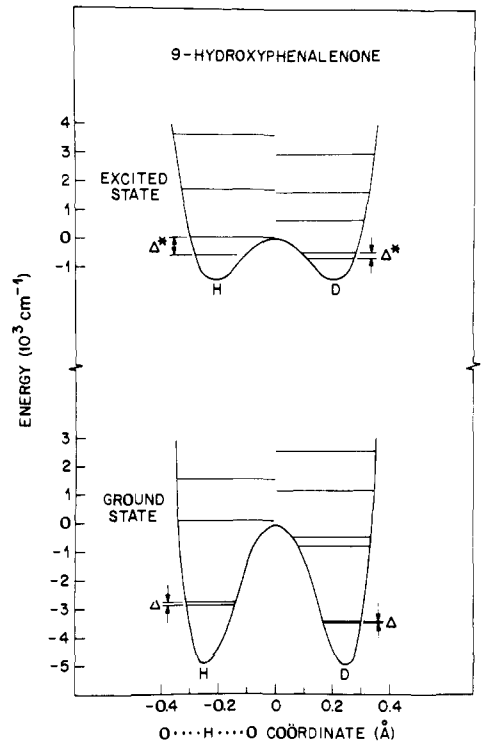

Figure 5. Calculated 9-HPO potential energy curves in both ground and excited states, based upon a simplified model discussed in the text. Quantized proton and deuteron vibrational levels are shown on the left and right sides, respectively.

modes. In this regard, we note that an OH stretch is absent from the IR spectra of 9-HPO;[18] the actual band may be unrecognizably broadened because of this strong coupling in v = 1.

The splittings Δ can be converted into the time domain if we adopt the model of proton coherent oscillation back and forth between the two wells. The transfer time τ is related to Δ via $\tau = h/2\Delta$, yielding τ(d) = 1.7 ps and τ(h) ≃ 0.13 ps in the ground electronic state. In the excited state, both τ(h) and τ(d) are less than 10^{-13} s.

Δ(d) increases by a factor of 19 in the excited state, while Δ(h) increases by a factor of ~5. As the barrier E_0 decreases in the excited state, the C_{2v} structure in Figure 1 assumes increasing importance in the electronic wave function. In somewhat loose language, the fluorescence of 9-HPO-*d* occurs from an excited state of mixed C_{2v}–C_s oxygen–carbon framework structure into a ground state of almost pure C_s structure. The normal mode A shown in Figure 2 probably converts the oxygen–carbon framework from C_s to C_{2v} and is strongly present in the 9-HPO-*d* emission for the reason discussed above. We suggest A is less prominent in 9-HPO-*h* emission as both excited and ground states contain substantial C_{2v} structure. This same argument should apply to the strong vibronic features in the excitation spectrum of 9-HPO-*d*.

The excited-state vibronic structure as seen in the excitation spectra of the 9-HPO-*h* seems totally transformed. We can speculate that the proton, vibrating almost at the top of the barrier in the excited state, actually undergoes a very complicated motion which strongly interacts with other modes. The O···H···O linear motion in Figure 5 may strongly couple with the other two-proton normal modes, producing a complicated three-dimensional oscillation. There might also be strong anharmonic coupling between O···H···O and the oxygen atom normal modes due to the fact that the proton at the top of the barrier undergoes a subtle balance of forces. ^{18}O isotopic substitution might prove informative.

Acknowledgment. We are grateful to F. H. Stillinger for stimulating discussions and for comments on the manuscript.

(16) For example, a CNDO/2 calculation of this effect in malonaldehyde has been carried out by S. Kato, H. Kato, and K. Fukui, *J. Am. Chem. Soc.*, **99**, 684 (1977).

(17) J. Laane, *Appl. Spectrosc.*, **24**, 73 (1970).

(18) Y. Demura, T. Kawato, H. Kanatomi, and I. Murase, *Bull. Chem. Soc. Jpn.*, **48**, 2820 (1975).